International Journal on Advanced Science Engineering Information Technology

Vol.13 (2023) No. 6
ISSN: 2088-5334

Analysis of 5.8 GHz Network for Line of Sight (LOS) and Non-Line of Sight (NLOS) in Suburban Environment

Ikha Fadzila Md Idris [a], Tan Kim Geok [b], Noor Ziela Abd Rahman [b,*], Mohd Haffizzi Md Idris [c]

[a] *Faculty of Business, Multimedia University, 75450, Melaka, Malaysia*
[b] *Faculty of Engineering and Technology, Multimedia University, 75450 Melaka, Malaysia*
[c] *Institute of Noise and Vibration Country, 54000 Kuala Lumpur, Malaysia*

*Corresponding author: *ziela.abdrahman@mmu.edu.my*

***Abstract*— This paper presents the findings of radio wave characterization based on the measurement data at 5.8 GHz. The measurement data were collected by a testbed channel, which links with the following scenarios: a single tree, a row of trees, a row of trees and a road, a row of trees, a road, and a building. These experiments were conducted at University Teknologi Malaysia (UTM) Skudai, Johor to represent the suburban environment. The links consist of pairs of transmitting and receiving antennas that deploy the path of a line of sight (LOS) and non-line of sight (NLOS) radio propagation wave networks. Based on the measurement data analysis, the general issue concerning the statistical probability distribution and the characteristics of LOS and NLOS are examined and discussed. Note that 5.8 GHz technology can be used in both LOS and NLOS scenarios, but its performance varies based on the presence of obstacles and signal propagation characteristics. Other prominent experimental analysis methods, such as hypothesis testing and goodness of fit tests, are implemented to consolidate the findings. The analysis found that the empirical probability density function of LOS and NLOS channels follows Gaussian, Rayleigh, and Rician distribution. Predicting specific future technological developments, such as the availability of 5.8 GHz technology, is challenging because it depends on various factors, including research and development efforts, regulatory decisions, market demand, and technological advancements.**

***Keywords*— Transmitter; receiver; radio wave propagation; line of sight; non-line of sight.**

Manuscript received 27 Nov. 2022; revised 15 Mar. 2023; accepted 18 Sep. 2023. Date of publication 31 Dec. 2022.

I. INTRODUCTION

Radio propagation is the behavior of radio waves propagating from one point to another, from a transmitting source or transmitter to a receiving antenna receiver. As the waves travel in the atmosphere, the radio signal may encounter reflection, diffraction, scattering, and absorption effects along the path [1], [2]. These are the prominent factors that affect radio wave propagation. As a result, the signal travel may be delayed, affecting the resultant signal. To thoroughly understand radio wave propagation characteristics, designing and optimizing wireless communication systems is important.

Line of sight (LOS) is one of the known propagation models where the radio waves travel in a straight line from the transmitter to the receiver. The propagation will not be smooth if any obstacle exists in its transmission path. Since the experiment is conducted in a suburban environment, in which the transmitter and receiver are mounted at the tree top level, the existence of trees will affect the received signal strength [3], [4]. In suburban environments, the signal strength gets attenuated easily, especially by significantly vegetated terrain and buildings. As a result, the transmitted signal tends to fade and encounter reflection and diffraction. This fading issue is addressed by configuring the appropriate statistical distribution and its characteristics. This study's targeted area is suburban in University Teknologi Malaysia (UTM) Skudai, Johor.

Unlike the line of sight (LOS) communication system, where the transmitter and receiver have a clear, unobstructed path, non-line of sight (NLOS) scenarios introduce additional challenges to wireless communication systems. In non-line-of-sight conditions, the radio waves may experience various propagation phenomena that cause the signal to deviate from the direct path, interacting with objects in the environment and taking multiple paths to reach the receiving antenna. As a result, the received signal may be weakened, distorted or subject to fading and interference [5], [6]. NLOS conditions

can occur in suburban environments with buildings, dense vegetation, or other physical structures that block or reflect the radio waves. Other environmental situations, such as indoor environments also exhibit NLOS characteristics where signals have to penetrate walls and obstacles. On top of that, conditions such as fog, rain, or atmospheric can contribute to NLOS propagation effects [7], [8].

The 5.8GHz frequency band is typically used for numerous wireless communications applications such as industrial, Wireless Fidelity (Wi-Fi), and amateur radio, as it offers clear advantages in terms of coverage and performance [9], [10]. The measurement campaign provides data analysis for the statistical distribution. Analysis enables researchers and analysts to organize, summarize, and interpret data meaningfully. Also, it is used to develop predictive models and make forecasts based on measured data. By identifying the patterns, parameters, and relationships in the data, statistical techniques can be used to invent models that project future trends and characteristics [11]–[13]. Based on work done in [12] and [14], the fading issue can be referred to as empirical characteristics of the statistical distribution. Other research work involving statistical analysis can be found, which depicts a statistical model for approximating LOS and NLOS probability in urban environments [15], [16],[17]. Other researchers also discovered that probability plays a crucial role in the proposed model for approximating the LOS probability and improving the accuracy of LOS probability approximation for 5G simulations [18], [19], [20], [21] and [22].

Signal interference, signal propagation, and optimizing the signal performance are the focuses of 5.8GHz analysis in suburban environments [6], [23], and [24]. To gauge this issue, statistical analysis [25] provides a systematic framework for extracting meaningful information from data, making sound decisions, and advancing knowledge in various disciplines [26]. The main objective of this paper is to investigate the characteristics and distribution of LOS and NLOS channels in suburban environments. On top of that, the work also investigates the analysis of statistical procedures, which are verified by the measurement results.

The following parts of this paper are organized as follows. Section II presents the statistical methodology related to the LOS and NLOS field that encompasses the techniques used in this paper. Results and Discussion are well described in Section III. To wrap up the work done, it will be explained in the last part of the paper in the conclusion section in Section IV.

II. Materials and Method

Prominent statistical distributions associated with radio wave propagation are well-known as Gaussian [27], Nakagami [28], Rayleigh and Rician [29] distributions. On top of that, all the parameters that describe the characteristics of the statistical distribution can be found in [30] and [31].

A. Gaussian distribution

Normal distribution or Gaussian distribution is an important continuous probability function in statistics. The random variable X has a Gaussian distribution if its probability density function is defined by [27]. It is called standard normal distribution when the parameters of $\mu = 1$ and $\sigma = 1$.

$$f(x) = \frac{1}{\sigma\sqrt{2\pi}} exp\left[-\frac{(x-\mu)^2}{2\sigma^2}\right], -\infty < x < \infty \quad (1)$$

where μ is the mean or location parameter
σ is the standard deviation

B. Rician distribution

Another continuous probability distribution function in wireless communication that is quite prominent is the Rician distribution. It is normally used to model density scattered signals that reach a receiver by multiple paths. The density function for Rician distribution is given by [29].

$$f(x) = \frac{x}{\sigma^2} exp\left[-\left(\frac{x^2+A^2}{2\sigma^2}\right)\right] I_0\left(\frac{xA}{\sigma^2}\right) \quad (2)$$

for $A \geq 0$ and $x \geq 0$

where x is the received envelope signals
I_0 is the zero-order modified Bessel function of the first kind.
σ^2 is the variance of random multipath component
A is the amplitude of the dominant component

C. Rayleigh distribution

In a condition where no LOS presence between both transmitter and receivers, Rayleigh distribution corresponds to model multipath propagation. It is also known as a special case of Weibull distribution with a scale parameter of 2. When a Rayleigh is set with a shape parameter of 1 ($\sigma = 1$, it is equal to a Chi-square distribution with a degree of freedom 2 [32]. The probability density function is represented in [33].

$$f(x) = \frac{x}{\sigma^2} exp\left[-\left(\frac{x^2}{2\sigma^2}\right)\right] \quad (3)$$

where x is the received envelope signals
σ^2 is the variance of random multipath component

D. Nakagami Distribution

Nakagami distribution is a generalized way to model small-scale fading for dense signal scatters in wireless signals. The Nakagami distribution is given by [28].

$$f(x) = \frac{2m^m}{\Gamma(m)\Omega^m} x^{(2m-1)} exp\left[-\left(\frac{mx^2}{\Omega}\right)\right] \quad (4)$$

where m is the shape parameter
x is the received envelope signals
Ω is the scale parameter
Γ is the gamma function

E. Weibull distribution

Weibull distribution is another useful tool to characterize outdoor multipath fading in wireless communication. The Weibull distribution is expressed in [30].

$$f(x) = a.b.x^{b-1} exp[-a.x^b] \quad (5)$$

where a is the scale parameter
b is the shape parameter

F. Lognormal distribution

In probability theory, a lognormal is a continuous probability distribution of a random variable whose logarithm

is normally distributed. A major difference is in its shape, the normal distribution is symmetrical whereas the lognormal distribution is not. Lognormal distribution can be expressed in [30].

$$f(x) = \frac{1}{x\sigma\sqrt{2\pi}} exp\left[-\frac{(\log(x)-\mu)^2}{2\sigma^2}\right] \quad (6)$$

where μ is the mean or location parameter
σ is the standard deviation.

All analytical measurements are made for links of transceivers. The receiver antenna's received signal strength (RSS) is measured in decibel units (dB). A total of thirteen pairs of links have been grouped into four categories, each representing the LOS and NLOS conditions. The first category that falls under LOS link is the obstructed link of the single tree category, which constitutes two pairs of transceivers. The second category under NLOS link is the the obstructed link of the row of trees with six pairs of transceivers. The third category representing the NLOS link is the obstructed link of a row of trees and roads with three pairs of transceivers. The last category that illustrates the NLOS link is the obstructed link of a row of trees, roads, and buildings, whereas this category has two pairs of transceivers.

Descriptive statistics are used to describe the characteristics and parameters of the measured data [34], [35], and [36]. It is practically used to check the variables for any violation of the statistical techniques' assumptions [37]. Apart from that, descriptive statistics provide information about the scores' distribution on continuous variables.

To obtain a statistical distribution, the statistical method of forecasting the received signal strength relies on measuring and averaging signal path loss for typical radio links. There are several procedures to verify the data distribution. As mentioned in [38], numerical methods, graphical methods (histogram and Q-Q plots), and formal normality test (Shapiro-Wilk) would be more stringent in addressing whether the data follows the normal probability distribution or well-known Gaussian distribution in the telecommunications field.

A normality test determines whether the sample has been drawn from a normally distributed population and involves numerous statistical tests. According to [39], the normality test is supplementary to the graphical assessment such as Kolmogorov-Smirnov test, Lilliefors, Shapiro-Wilk test, Anderson Darling test, etc. Even though several prominent normality tests have been conducted in research, the Shapiro-Wilk has been justified as the most powerful normality test [38].

In the hypothesis testing procedure [40], there will be two assumptions to determine whether the data follows the normal distribution. These assumptions are typically known as hypothesis testing where:

- H_0 : the data is normally distributed
- H_a : the data is not normally distributed.

Note: null hypothesis is denoted as H_0, and alternative hypothesis is denoted as Ha.

Hence, if the p-value is less than the predefined significance level, as stated in [41], the null hypothesis is rejected, and there is evidence that the data tested are not normally distributed. Apart from findings in [42], typically Kolmogorov-Smirnov (KS) test and Shapiro-Wilk would depend on the data analysis's sample size. This KS test measures the largest discrepancy between the two distributions and computes the p-value, indicating the goodness of fit.

It is essential to note that the method above provides indications or evidence of whether the data follows a Gaussian distribution [43]. In summary, a combination of visual inspection of histogram, Quantile-Quantile or Q-Q plots [44], a statistical test of goodness of fit and consideration of descriptive statistics can help assess whether the data follows a Gaussian distribution [43] and [45]. The Rayleigh distribution is generally used to model the magnitude of a vector whose components are independently and identically distributed Gaussian random variables [46]. In a Rayleigh distribution, the histogram exhibits a skewed shape, with a long tail on the right side. The density plot may resemble a smooth, decreasing curve. Rician distribution is commonly used to model the amplitude of a signal in a wireless communication system where there is a dominant line of sight component combined with scattered or reflected waves. In a Rician distribution, the data typically exhibits a peaked or bimodal shape, with a prominent peak at a non-zero value representing the data component.

In order to analyse the characteristics of the signal, the measurement results are presented through descriptive analysis and graphical display. The hypothesis testing procedure is then performed to validate the analysis. Finally, the parameters of the statistical distribution that best fit the results are extracted.

III. Results and Discussion

According to [47], the graphical distribution will contribute to the symmetric distribution if the mean value is equivalent to the median value. The symmetry shows that these two data sets' transceivers follow the Gaussian distribution.

The descriptive statistics in Table 1 show that the mean and median value for LOS link (MA7_MA10 and K11_K28) of the single tree category is equivalent, indicating that the distribution's shape is normal curve or bell shape. This supports that the two links under single tree category follow the Gaussian distribution. For NLOS, under a row of trees category, three links; K01_K16, K11_K23 and K11_K24 exhibit the normal shape of Gaussian distribution as they have the same mean and median value.

On the contrary, links K01_K17, M01_M19 and L01_L34 show that mean and median values are not equivalent. This reflects that these three links are not considered Gaussian distribution, which might lead to deploying other statistical distributions with different parameters and characteristics. For other categories in NLOS, only one pair of transceivers, link MA1_MA38 is said to follow the Gaussian distribution since the consistency value of mean and median leads to the bell-shape curve. Linking MA1_MA23 and MA1_M42 in a row of trees and road categories show the inconsistency value of mean and median; hence, it does not comply with the Gaussian distribution. The last category of a row of trees, roads, and buildings, shows that the K11_K26 link has a different value of mean and median, which tells us that it does not have the normal curve and does not follow the Gaussian curve, which contradicts link K11_K22.

Normalizing data from zero to one will follow the standardization of a normal curve that can fit the normal distribution. Considering that graphical displays are one of the visualization techniques to validate the data, graphical displays of every link are shown in the following diagrams. In Fig. 1(a), the LOS follows the Gaussian distribution for link MA7_MA10. It is proven by the Q-Q plot in Fig. 1 (b), which shows that the data points fall approximately along a straight line. Thus, this indicates that the data closely follows Gaussian distribution.

In Fig. 2(a), the LOS shows that it does not follow the Gaussian distribution (as described by referring to the descriptive statistics table). Since the graph portrays few peaks and has a long tail skewed to the right of the graph in a decreasing curve, the suitable distribution that fits to this link K11_K28 is Rayleigh distribution. To support this statement, the Q-Q plot in Fig. 2 (b) shows that the data points do not fall approximately along a straight line. This characteristic does not meet the earlier assumption on the mean and median equivalency findings in Table 1. The existence of blockages leads to the propagation of radio waves and scattering and reflection. The environmental effect greatly impacts this channel of receiving antenna networks.

In Fig. 3(a), Fig. 5(a), Fig. 6(a), and Fig. 8(a), the link K01_K16, K11_K23, K11_K24, and L01_L34 follows the Gaussian distribution since it shows the smooth curve in the PDF graph and the skewness is balanced on left and right. The Q-Q plot in Fig. 3(b), Fig. 5(b), Fig. 6(b), and Fig. 8(b) also shows that the data points fall approximately along a straight line; this indicates that the data closely follows Gaussian distribution.

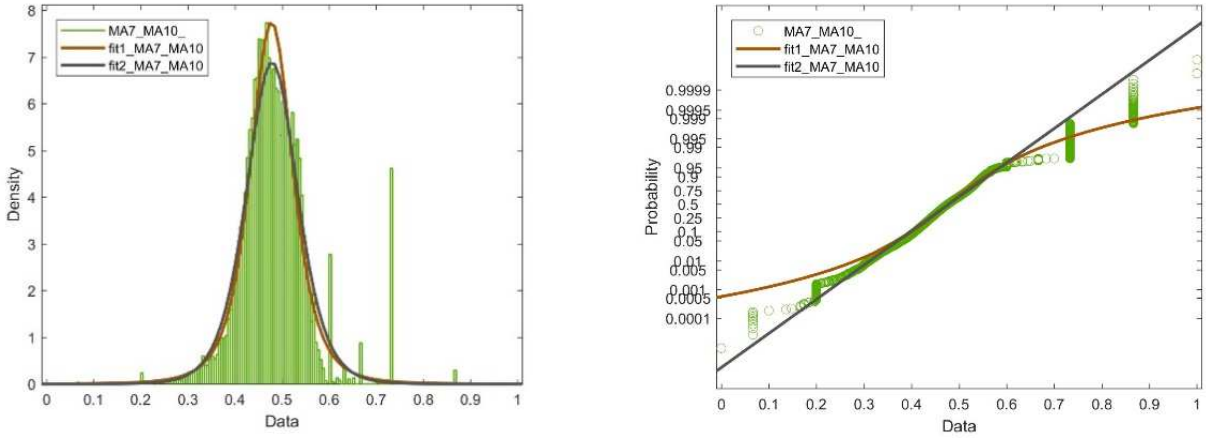

(a) (b)

Fig. 1 (a). PDF graph (b) Probability plot for link MA7_MA10 LOS (Single tree category)

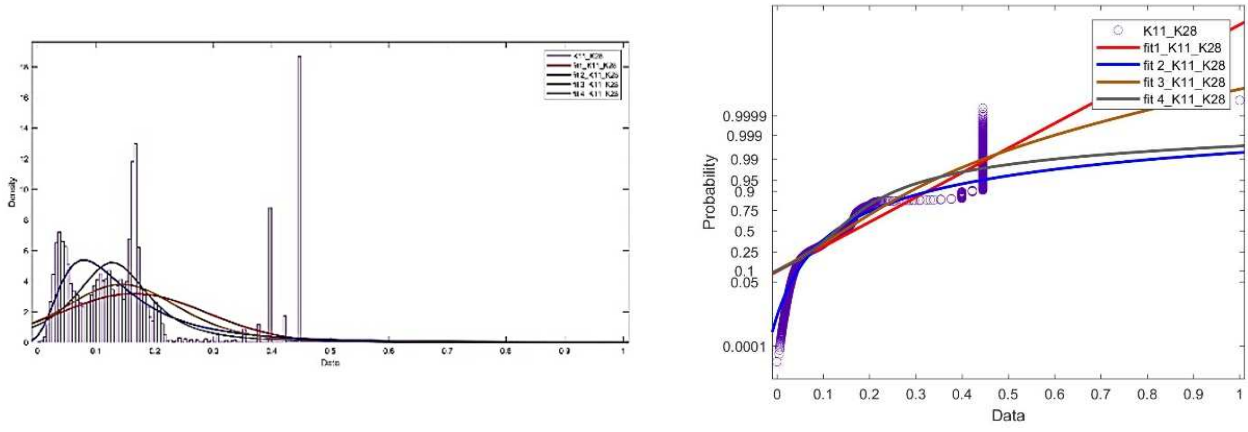

(a) (b)

Fig. 2 (a). PDF graph (b) Probability plot for link K11_K28 LOS (Single tree category)

Link L01_L34, in the beginning, obtained almost equivalent values of mean and median, as shown in the descriptive statistics. However, it should be supported with these graphical diagrams. For this scenario, wave propagation attenuates when the signal travels from one point to another due to the wave traveling to multipath propagation.

For NLOS link in Fig. 4(a), the link of K01_K17 follows a Rician distribution due to the bimodal shape. The Q-Q plot in Fig. 4(b) also shows that the data points fall approximately along a straight line, which later, we will consolidate the finding with access to the statistical goodness of fit test.

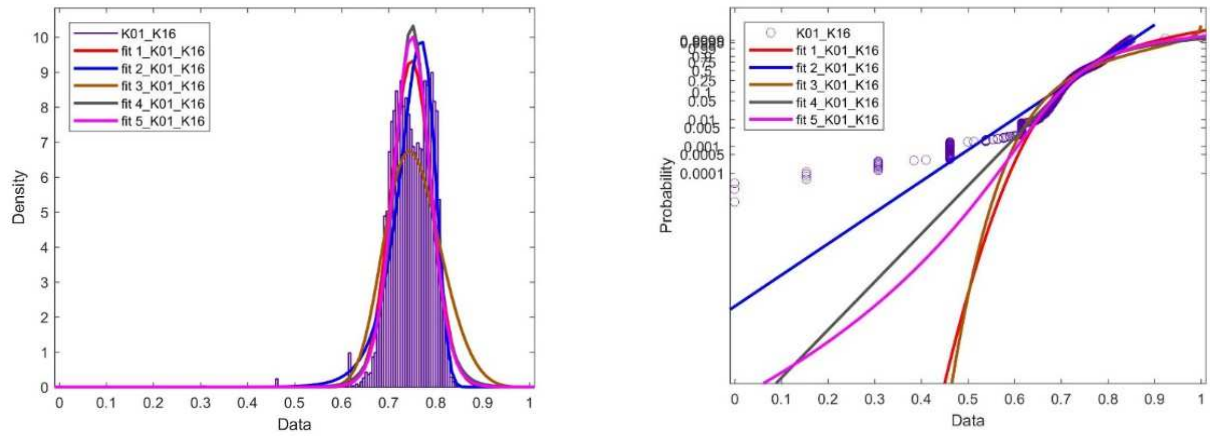

(a) (b)

Fig. 3 (a). PDF graph (b) Probability plot for K01_K16 NLOS (Row of trees category)

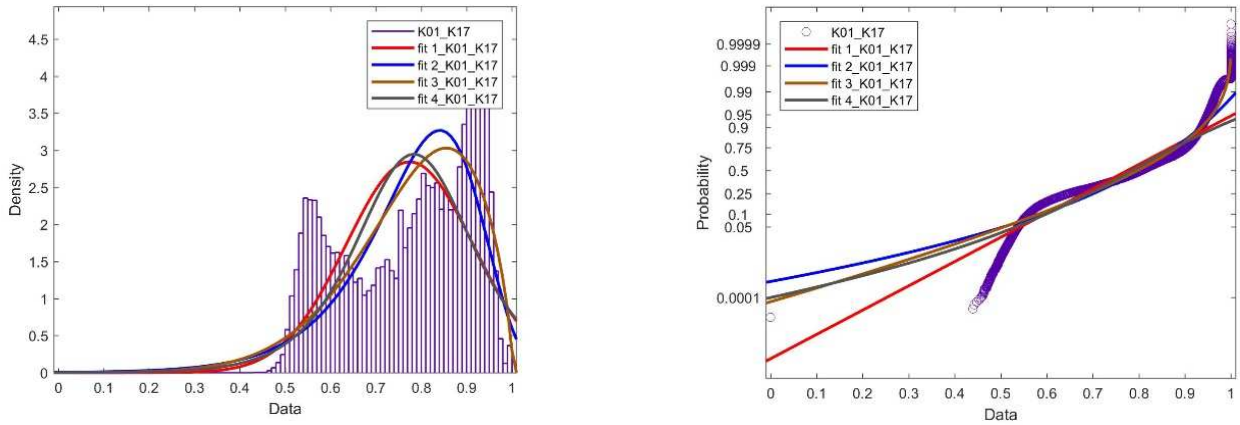

(a) (b)

Fig. 4 (a). PDF graph (b) Probability plot for link K01_K17 NLOS (Row of trees category)

In Fig. 3(a), Fig. 5(a), Fig. 6(a), and Fig. 8(a), the link K01_K16, K11_K23, K11_K24 and L01_L34 follows the Gaussian distribution since it shows the smooth curve in the PDF graph and the skewness is balanced on left and right. The Q-Q plot in Fig. 3(b), Fig. 5(b), Fig. 6(b), and Fig. 8(b), also shows that the data points fall approximately along a straight line. This indicates that the data closely follows Gaussian distribution.

Link L01_L34, in the beginning, obtained almost equivalent values of mean and median, as shown in the descriptive statistics. However, it should be supported with these graphical diagrams. For this scenario, wave propagation attenuates when the signal travels from one point to another due to the wave traveling to multipath propagation.

For NLOS link in Fig. 4(a), the link of K01_K17 follows a Rician distribution due to the bimodal shape. The Q-Q plot in Fig. 4(b) also shows that the data points fall approximately along a straight line, which later, we will consolidate the finding with access to the statistical goodness of fit test.

In Fig. 7(a), the NLOS link M01_M19 shows that it does not follow the Gaussian distribution (as described by referring to the descriptive statistics table). The decreasing curve of right skewness tells that this link best suits with Rayleigh distribution. On top of that, the Q-Q plot shows that the data points do not fall approximately along a straight line in Fig. 7(b). The blockage could affect the received signal strength that can be scattered and reflected before the transmitter can reach the receiver.

For NLOS link in Fig. 9(a) and Fig. 11(a), the link of MA1_MA23 and MA1_MA42 follows a Rician distribution due to the bimodal shape of the distribution. The Q-Q plot in Fig. 9(b) and Fig. 11(b) also shows that the data points fall approximately along a straight line, which later, we will validate the finding with access to statistical goodness of fit test. Fig. 10(a) shows that it follows the Gaussian distribution for link MA1_MA38. In addition, the Q-Q plot in Fig. 10(b) shows that the data points fall approximately along a straight line of the observed value. Thus, this implies that the data closely follows Gaussian distribution.

TABLE I
DESCRIPTIVE STATISTICS SUMMARY FOR ALL LINKS

Category	Single Tree		Row of Trees						Row of Trees and Road			Row of Trees, Road and Building	
Links	**MA7_ MA10**	**K11_ K28**	**K01_ K16**	**K01_ K17**	**K11_ K23**	**K11_ K24**	**M01_ M19**	**L01_ L34**	**MA1_ MA23**	**MA1_ MA38**	**MA1_ M42**	**K11_ K22**	**K11_ K26**
Minimum	-62.538	-84.784	-63.242	-75.811	-75.667	-93.500	-87.672	-61.329	-77.000	-72.634	-84.788	-86.347	-68.500
Maximum	-59.964	-62.800	-61.000	-74.470	-63.950	-84.000	-85.154	-59.403	-70.875	-67.979	-81.600	-82.000	-59.583
Range	2.575	21.984	2.242	1.341	11.717	9.500	2.518	1.927	6.125	4.655	3.188	4.347	8.917
1st Quartile	-61.120	-83.518	-62.552	-75.212	-67.378	-87.375	-86.594	-60.407	-75.825	-70.211	-83.287	-84.865	-62.250
Median	-60.875	-82.133	-61.849	-74.941	-66.500	-87.019	-86.152	-60.238	-74.463	-69.758	-83.178	-84.170	-61.726
3rd Quartile	-60.605	-81.167	-61.299	-74.830	-65.815	-86.634	-85.879	-60.000	-74.067	-69.198	-83.040	-83.774	-61.122
Mean	-60.876	-82.199	-61.844	-74.922	-64.696	-87.067	-86.240	-60.263	-76.413	-69.761	-83.185	-84.178	-62.746
Variance (n-1)	0.117	1.972	0.415	0.063	1.390	0.804	0.177	0.108	0.935	0.524	0.168	0.533	0.708
Standard deviation (n-1)	0.341	1.404	0.645	0.252	1.179	0.896	0.420	0.328	0.967	0.724	0.410	0.730	0.841
Skewness (Pearson)	-0.300	0.782	-0.562	-0.685	-1.417	-1.944	-0.394	-0.606	-0.032	-0.570	0.885	-0.133	-1.742
Kurtosis (Pearson)	-0.258	2.820	-1.363	-0.590	3.883	5.572	-0.952	-0.270	-0.645	-0.197	1.665	-0.596	8.921
Standard error of the mean	0.002	0.007	0.003	0.001	0.006	0.005	0.002	0.002	0.005	0.004	0.002	0.004	0.004

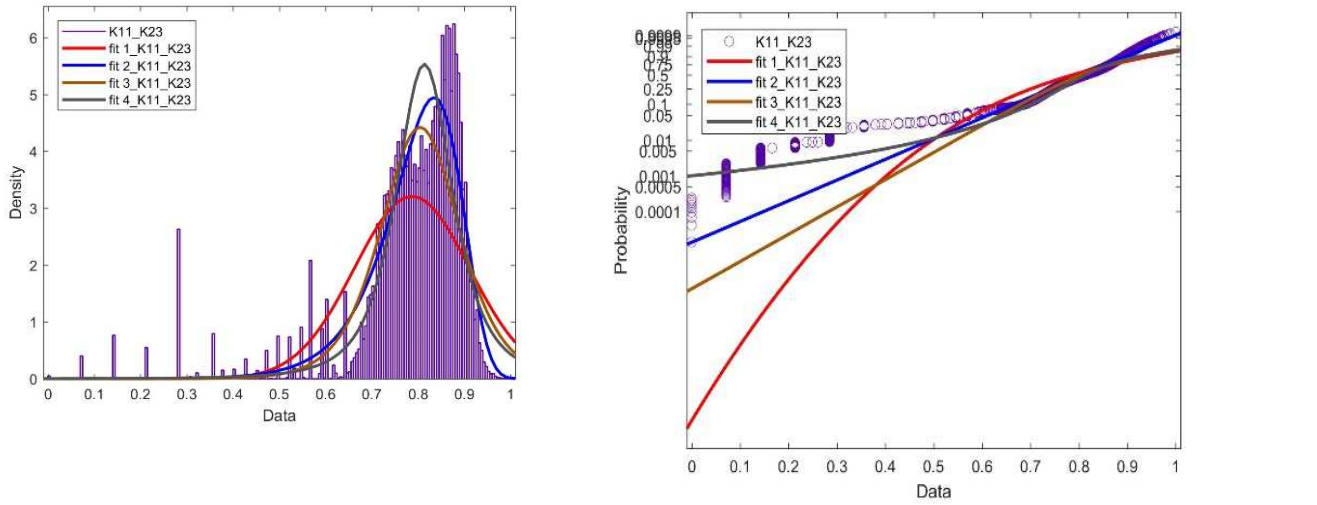

(a) (b)

Fig. 5 (a). PDF graph (b) Probability plot for link K11_K23 NLOS (Row of trees category

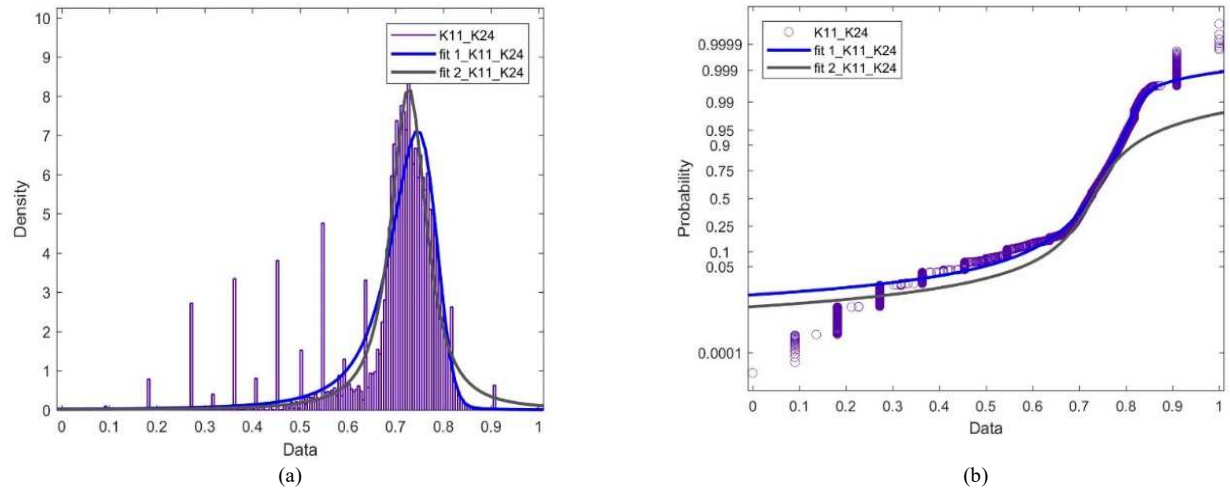

(a) (b)

Fig. 6 (a). PDF graph (b) Probability plot for link K11_K24 NLOS(Row of trees category)

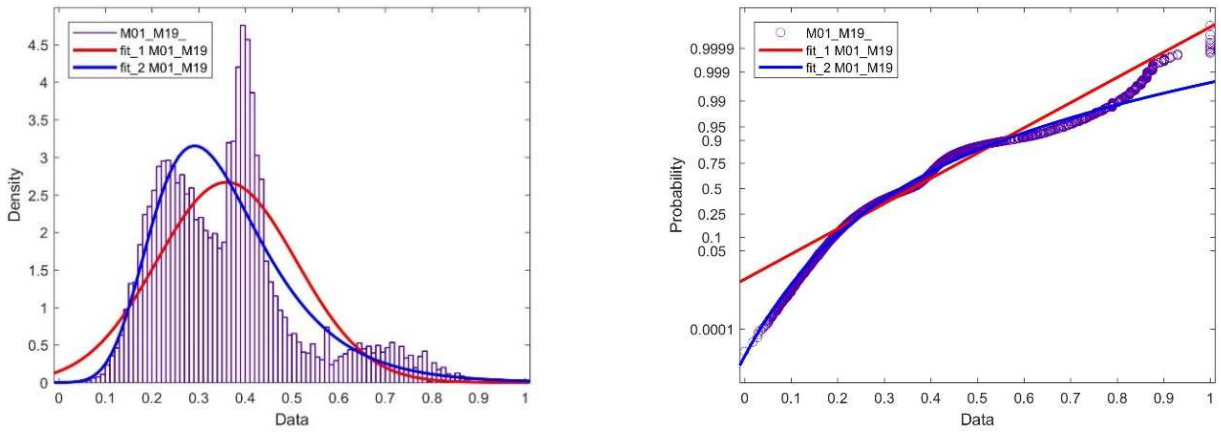

(a) (b)

Fig. 7 (a). PDF graph (b) Probability plot for link M01_M19 NLOS (Row of trees category)

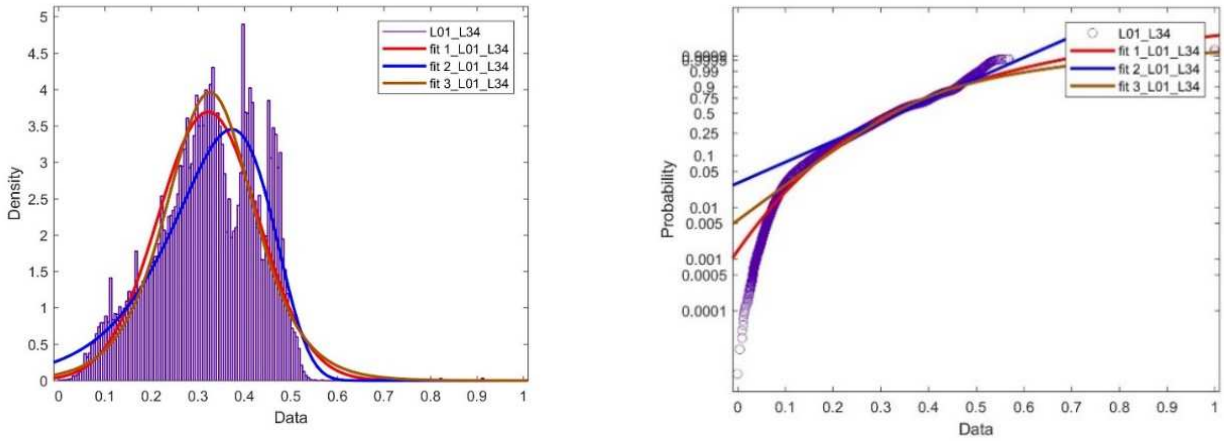

(a) (b)

Fig. 8 (a). PDF graph (b) Probability plot for link L01_L34 NLOS (Row of trees category)

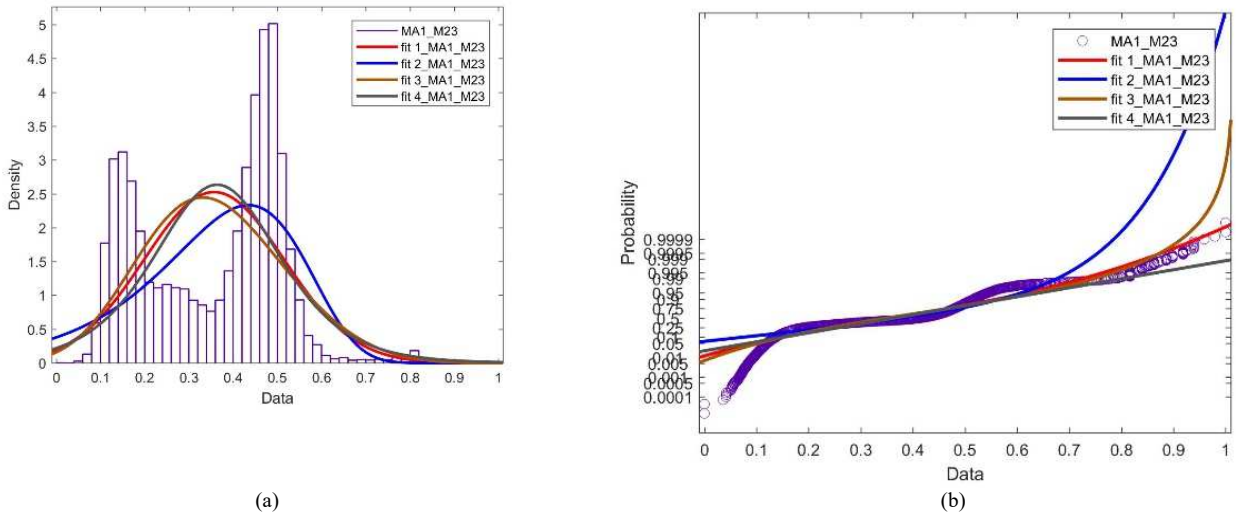

(a) (b)

Fig. 9 (a). PDF graph (b) Probability plot for link MA1_MA23 NLOS (Row of trees and road category)

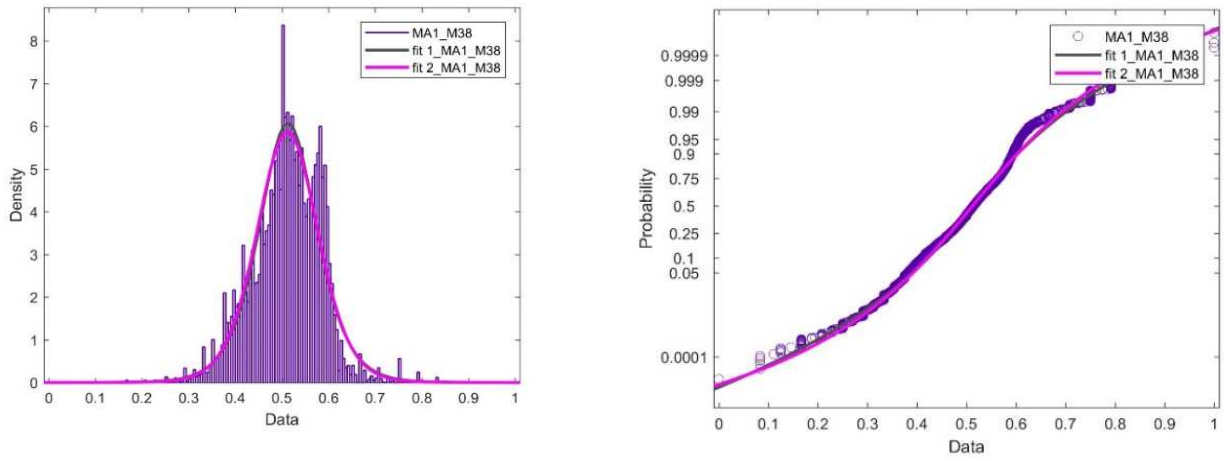

(a) (b)

Fig. 10 (a). PDF graph (b) Probability plot for link MA1_MA38 NLOS (Row of trees and road category)

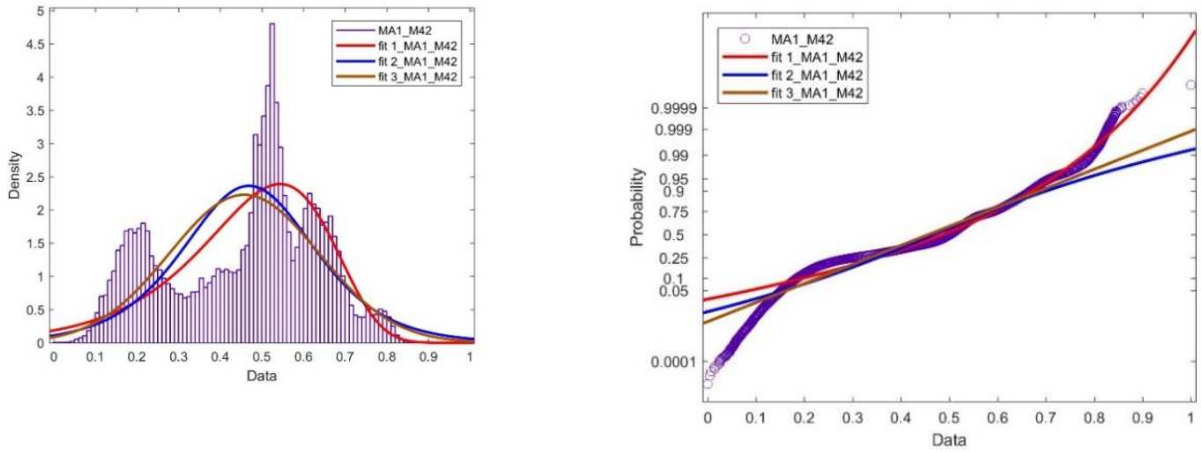

(a) (b)

Fig. 11 (a). PDF graph (b) Probability plot for link MA1_MA42 NLOS (Row of trees and road category

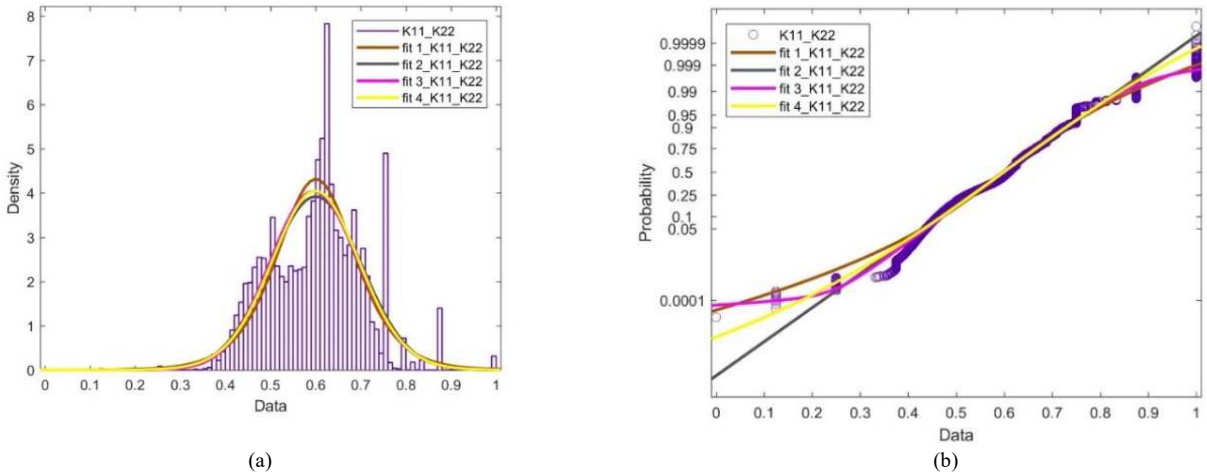

(a) (b)

Fig. 12 (a). PDF graph (b) Probability plot for link K11_K22 NLOS (Row of trees, road and building category)

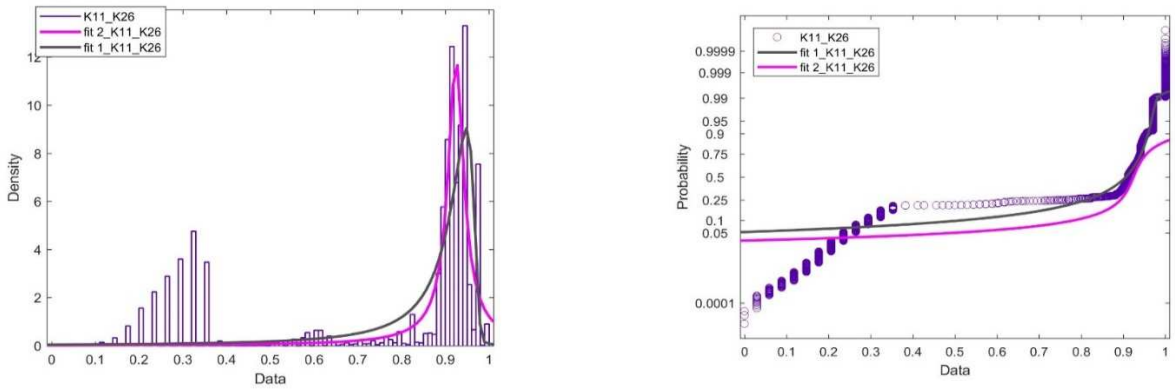

Fig. 13 (a). PDF graph (b) Probability plot for link K11_K26 NLOS (Row of trees, road and building category)

For NLOS link in Fig. 12(a) shows that it follows the Gaussian distribution for link K11_K22. In addition, the Q-Q plot in Fig. 12(b) shows that the data points fall approximately along a straight line of the observed value. Thus, this implies that the data closely follows Gaussian distribution. While in Fig. 13(a), the link of K11_K26 follows a Rician distribution due to the bimodal shape of the distribution. The Q-Q plot in Fig. 13(b) also shows that the data points fall approximately along a straight line, which later, we will validate the finding with access to statistical goodness of fit test.

Table 2 shows the p-value of the normality test conducted on these thirteen obstructed links of LOS and NLOS. The normality test consists of the Shapiro-Wilk, AD or Anderson-Darling, Lilliefors, and Jarque-Bera tests. Only six transceiver links give the p-value less than 0.0001, implying that it is less than the 0.05 significance level. We shall reject the null hypothesis and can conclude that the data do not follow the continuous probability of Gaussian distribution. The six links are K11_K28 from the single tree category, K01_K17, and M01_M19 from a row of trees category, MA1_MA23 and MA1_M42 from a row of trees and road category, and the last category from a row of trees, road, and building is link K11_K26.

TABLE II
P-VALUE OF NORMALITY TEST

		Normality Test (p-value)			
Category	**Link**	**Shapiro-Wilk**	**Anderson-Darling**	**Lilliefors**	**Jarque-Bera**
Single tree	MA7_MA10	0.0783	0.0831	0.0684	0.0673
	K11_K28	<0.0001	<0.0001	<0.0001	<0.0001
Row of trees	K01_K16	0.0881	0.0784	0.0888	0.081
	K01_K17	<0.0001	<0.0001	<0.0001	<0.0001
	K11_K23	0.0544	0.0842	0.0670	0.0883
	K11_K24	0.0515	0.0902	0.1009	0.2000
	M01_M19	<0.0001	<0.0001	<0.0001	<0.0001
	L01_L34	0.0698	0.0765	0.0575	0.0532
Row of trees and road	MA1_MA23	<0.0001	<0.0001	<0.0001	<0.0001
	MA1_MA38	0.0977	0.0925	0.0800	0.0810
	MA1_M42	<0.0001	<0.0001	<0.0001	<0.0001
Row of trees, road and building	K11_K22	0.0787	0.0786	0.1041	0.2012
	K11_K26	<0.0001	<0.0001	<0.0001	<0.0001

TABLE III
ESTIMATED PARAMETERS OF OBSTRUCTED LINKS FOR FOUR DIFFERENT CATEGORIES

Category	**Link**	μ	σ	k	**Distribution**
Single tree	MA7_MA10	0.478852	0.0362667	-	Gaussian
	K11_K28	0.163992	0.125467	-	Rayleigh
Row of trees	K01_K16	0.77452	0.140196	-	Gaussian
	K01_K17	0.748924	0.042702	0.00435165	Rician
	K11_K23	0.786666	0.124406	-	Gaussian
	K11_K24	0.695151	0.110552	-	Gaussian
	M01_M19	0.29202	0.116698	-	Rayleigh
	L01_L34	0.322032	0.108039	-	Gaussian
Row of trees and road	MA1_MA23	0.924248	0.0241578	0.642315	Rician
	MA1_MA38	0.510358	0.0736887	-	Gaussian
	MA1_M42	0.457837	0.179111	0.256189	Rician
Row of trees, road and building	K11_K22	0.60001	0.101755	-	Gaussian
	K11_K26	0.03395	0.961345	0.79613	Rician

Radio waves can interfere with each other when multiple signals occupy the same frequency band or when reflected or diffracted waves arrive at the receiver at slightly different times. In short, this interference degrades the quality and reliability of wireless communications and is an important consideration in system design. The decision rule of the p-value obtained is more than five percent of the significant level, suggesting that the null hypothesis is accepted [41]. It can be interpreted that the remainder of the links obey the Gaussian distribution. It is essential to note that maximum likelihood estimation or MLE assumes that the data are independent and identically distributed (i.i.d) and that the chosen probability distribution accurately represents the underlying data-generating process. The estimated parameters measure the probability of observing data under the assumed models. Table 3 presents the estimated parameter values and statistical distributions of LOS and NLOS channels. The data in Table 3 supports and consolidates the findings of the statistical distribution function.

IV. CONCLUSION

The link that follows the Gaussian distributions under LOS occurs for link MA7_MA10. For NLOS channels, which cover different categories of obstructed channels, constitute of six links that comply to the Gaussian are K01_K16, K11_K23, K11_K24, L01_L34, MA1_MA38 and K11_K22. The link K11_K28 under LOS category follows the Rayleigh distribution. As for NLOS network channels, only link M01_M19 obeys the Rayleigh distribution. The remaining links exhibit the Rician characteristics are K01_K17, MA1_MA23, MA1_M42, and K11_K26. In this study, the radio link of LOS and NLOS is measured and examined concerning how the propagation of 5.8GHz channel frequency affects the different categories of obstructed path.

In view to the characteristics of the experimental measurement, a statistical model for LOS and NLOS is proposed to improve the accuracy concerning deterministic estimation. Approximation could be applied to other types of known LOS and NLOS probability functions and more statistical tests that enable the researcher to reach more quantitative results.

ACKNOWLEDGMENT

The authors thank Multimedia University, Prof. Dr. Tharek bin Abd Rahman, and Wireless Communication Center, Universiti Teknologi Malaysia, for providing intensive assistance to this research. This paper is funded by the Ministry of Education, FRGS/1/2014/TK03/MMU/03/3 grant number.

REFERENCES

[1] R. Dangi, P. Lalwani, G. Choudhary, I. You, and G. Pau, "Study and Investigation on 5G Technology: A Systematic Review," *Sensors 2022*, vol. 26, no. 22, 2022. doi:10.3390/s22010026.

[2] A. Sufyan, K. B. Khan, O. A. Khashan, T. Mir, and U. Mir, "From 5G to beyond 5G: A Comprehensive Survey of Wireless Network Evolution, Challenges, and Promising Technologies," *Electron. 2023*, vol. 12, no. 10, p. 1200, 2023. doi:10.3390/electronics12102200.

[3] T. Hsiung and Y. Kanza, "SimCT: Spatial Simulation of Urban Evolution to Test Resilience of 5G Cellular Networks," in *Proceedings of the 2nd ACM SIGSPATIAL International Workshop on GeoSpatial Simulation*, 2019, pp. 1–8. doi:10.1145/3356470.3365526.

[4] J. Du, D. Chizhik, and R. Feick, "Suburban Fixed Wireless Access Channel Measurements and Models at 28 GHz for 90% Outdoor Coverage," *IEEE Trans. Antenna Propag.*, vol. 68, no. 1, pp. 411–421, 2020. doi:10.1109/TAP.2019.2935110.

[5] M. M. Khan, "Design and Analysis of a Compact UWB Band Notch Antenna for Wireless Communication," *Eng. Proc. 3*, vol. 1, no. 6, pp. 1–6, 2020. doi:10.3390/IEC2020-06974.

[6] W. Peng, X. Li, H. Zhang, Z. Liu, and W. Song, "A 5.8 GHz high-gain flexible receiving antenna for wireless power transmission," *AIP Adv.*, vol. 12, no. 12, 2022. doi:10.3390/IEC2020-06974.

[7] N. Z. A. Rahman, T. K. Geok, T. A. Rahman, I. F. M. Idris, and N. A. A. Hamzah, "Modeling of Dynamic Effect of Vegetation for Fixed Wireless Access," *Wirel. Pers. Commun.*, vol. 96, no. 1, pp. 709–728, 2017. doi:10.1007/s11277-017-4240-1.

[8] Q. Hou, M. Chai, and H. Wang, "Dynamic modeling of traffic noise in both indoor and outdoor environments by using a ray tracing method," *Build. Environ.*, vol. 121, pp. 225–237, 2017. doi:10.1016/j.buildenv.2017.05.031.

[9] Y. H. Santana, R. M. Alonso, G. G. Nieto, L. Martens, W. Joseph, and D. Plets, "Indoor Genetic Algorithm-Based 5G Network Planning Using a Machine Learning Model for Path Loss Estimation," *J. Appl. Phys.*, vol. 12, p. 3923, 2022. doi:10.3390/app12083923.

[10] N. Shabbir *et al.*, "Vision towards 5G: Comparison of radio propagation models for licensed and unlicensed indoor femtocell sensor networks," *Phys. Commun.*, vol. 47, pp. 1–11, 2021. doi:10.1016/j.phycom.2021.101371.

[11] K. Haneda *et al.*, "Radio propagation modeling methods and tools," in *Inclusive Radio Communications for 5G and Beyond*, 2021, pp. 7–48. doi:10.1016/B978-0-12-820581-5.00008-0.

[12] N. Rajesh *et al.*, "Statistical Characterization and Modeling of Radio Frequency Signal Propagation in Mobile Broadband Cellular Next Generation Wireless Networks," *Comput. Intell. Neurosci.*, 2023. doi:10.1155/2023/5236566.

[13] S. K. . R. Wickramasinghe and K. A. Razak, "The Impact of The Telecommunication Industry as a Moderator on Poverty Alleviation and Educational Programmes to Achieve Sustainable Development Goals In Developing Countries," *J. Informatics Web Eng.*, vol. 2, no. 1, pp. 25–37, 2023. doi:10.33093/jiwe.2023.2.1.3.

[14] J. M. Romero-Jerez, F. J. Lopez-Martinez, J. F. Paris, and A. J. Goldsmith, "The Fluctuating Two-Ray Fading Model: Statistical Characterization and Performance Analysis," *IEEE Trans. Wirel. Commun.*, vol. 16, no. 50, pp. 4420–4432, 2017. doi:10.1109/TWC.2017.2698445.

[15] R. Aleksiejunas, "Statistical Approximations of LOS/NLOS Probability in Urban Environment," *ArXiv*, vol. abs/2001.1, 2020. doi:10.48550/arXiv.2001.11813.

[16] N. Díaz, J. Guerra, M. Freire, and J. C. Aviles, "Vehicle Blocking Effect in an Urban NLOS Radio Link Operating in the 28 GHz Band," in *2019 IEEE 2nd International Conference on Electronics and Communication Engineering*, 2019, pp. 133–138. doi:10.48550/arXiv.2001.11813.

[17] M. D. Buhari, T. B. Susilo, I. Khan, and B. O. Sadiq, "Statistical LOS/NLOS Classification for UWB Channels," *KIU J. Sci. Eng. Technol.*, vol. 2, no. 1, 2023. doi:10.48550/arXiv.2001.11813.

[18] R. Aleksiejunas, A. Cesiul, and K. Svirskas, "Statistical LOS/NLOS Channel Model for Simulations of Next Generation 3GPP Networks," *Elektron. IR ELEKTROTECHNIKA*, vol. 24, no. 5, pp. 74–79, 2018. doi:10.5755/j01.eie.24.5.21847.

[19] C. G. Ruiz, A. Pascual-Iserte, and O. Munoz, "Analysis of Blocking in mmWave Cellular Systems: Characterization of the LOS and NLOS Intervals in Urban Scenarios," *IEEE Trans. Veh. Technol.*, vol. 69, no. 12, pp. 16247–16252, 2020. doi:10.1109/TVT.2020.3037125.

[20] I. Mohammed, S. Gopalam, I. B. Collings, and S. V. Hanly, "Closed Form Approximations for UAV Line-of-Sight Probability in Urban Environments," *IEEE Access*, vol. 11, pp. 40162–40174, 2023. doi:10.1109/ACCESS.2023.3267808.

[21] M. K. Samimi and T. S. Rappaport, "3-D Millimeter-Wave Statistical Channel Model for 5G Wireless System Design," *IEEE Trans. Microw. Theory Tech.*, vol. 64, no. 7, pp. 2207–2220, 2016. doi:10.1109/TMTT.2016.2574851.

[22] Muhammad Zeeshan Asghar, S. A. Memon, and J. Hämäläinen, "Evolution of Wireless Communication to 6G: Potential Applications and Research Directions," vol. 14, no. 10, p. 6356, 2022. doi:10.3390/su14106356.

[23] M. Quispe, J. Olivares, J. Samaniego, and R. Morán, "Technical and economic analysis of TVWS and 5.8 GHz Wi-Fi systems for rural areas," in *2022 IEEE XXIX International Conference on Electronics,*

Electrical Engineering and Computing (INTERCON), 2022, pp. 1–4. doi:10.1109/INTERCON55795.2022.9870159.

[24] C. Sudhamani, M. Roslee, L. L. Chuan, A. Waseem, A. F. Osman, and M. H. Jusoh, "Performance Analysis of a Millimeter Wave Communication System in Urban Micro, Urban Macro, and Rural Macro Environments," *J. Energies*, vol. 16, no. 14, p. 5358, 2023. doi:10.3390/en16145358.

[25] H. Kou, "Wireless Communication System and Its Application in Big Data Remote Monitoring and Decision-Making," vol. 2022, p. 10, 2022. doi:10.1155/2022/8161917.

[26] W. Yu, F. Sohrabi, and T. Jiang, "Role of Deep Learning in Wireless Communications," vol. 2, no. 2, pp. 56–72, 2022. doi:10.1109/MBITS.2022.3212978.

[27] M. Chai and J. Yang, "Parameter estimation of network signal normal distribution applied to carbonization depth in wireless networks," *EURASIP J. Wirel. Commun. Netw.*, vol. 2020, no. 1, pp. 1–15. doi:10.1186/s13638-020-01694-5.

[28] F. Yilmaz, M. O. Hasna, and K. Qaraqe, "Alternative expressions of the PDF and CDF for Gamma, η−μ and κ−μ shadowed distributions," *Phys. Commun.*, vol. 56, 2023. doi:10.1016/j.phycom.2022.10.

[29] J. W. Browning, S. L. Cotton, D. Morales-Jimenez, and D. Morales-Jimenez, "The Rician Complex Envelope Under Line of Sight Shadowing," *IEEE Commun. Lett.*, vol. 12, no. 2182–2186, 2019. doi:10.1109/LCOMM.2019.2939304.

[30] A. T. Adeniran, O. Faweya, T. O. Ogunlade, and K. O. Balogun, "Derivation of Gaussian Probability Distribution: A New Approach," *Appl. Math.*, vol. 11, no. 6, pp. 436–446, 2020. doi:10.1109/LCOMM.2019.2939304.

[31] A. Dmitriev, A. Ryzhov, and C. Sierra-Teran, "Statistical Characteristics of Differential Communication Scheme Based on Chaotic Radio Pulses," *Electron. 2023*, vol. 12, no. 6, p. 1495, 2023. doi:10.3390/electronics12061495.

[32] Y. Chen, D. Zhang, and Q. Zhu, "Markov chain modelling of ordered Rayleigh fading channels in non-orthogonal multiple access wireless networks," *IET Signal Process.*, vol. 17, no. 3, p. 11, 2023. doi:10.1049/sil2.12191.

[33] H. M. Almongy, E. M. Almetwally, H. M. Aljohani, A. S. Alghamdi, and E. H. Hafez, "A new extended rayleigh distribution with applications of COVID-19 data," *Results Phys.*, vol. 23, pp. 1–9, 2021. doi:10.1016/j.rinp.2021.104012.

[34] S. Mendonça, B. Damásio, L. C. de Freitas, L. Oliveira, M. Cichy, and A. Nicita, "The rise of 5G technologies and systems: A quantitative analysis of knowledge production," *Sci. Direct*, vol. 46, no. 4, p. 102327, 2022. doi:10.1016/j.telpol.2022.102327.

[35] D. Bajoivć, B. Sinopoli, and Joã, "Sensor selection for hypothesis testing in wireless sensor networks: a Kullback-Leibler based approach," in *IEEE Conference on Decision and Control*, 2009, pp. 1659–1664. doi:10.1109/CDC.2009.5400743.

[36] D. Passos, F. G. O. Passos, B. dos S. Silva, and C. Albuquerque, "Modeling the performance of the link quality hypothesis test estimator mechanism in wireless networks," *Wirel. Networks*, vol. 27, pp. 4065–4081, 2021. doi:10.1080/03610926.2021.1977961.

[37] M. Walter and M. Schnell, "Statistical distribution of line-of-sight and reflected path in the aeronautical channel," in *2011 IEEE/AIAA 30th Digital Avionics Systems Conference*, 2011, pp. 4D1-1-. doi:10.1109/DASC.2011.6095909.

[38] M. Saculinggan and E. A. Balase, "Empirical Power Comparison Of Goodness of Fit Tests for Normality In The Presence of Outliers," *J. Phys. Conf. Ser.*, vol. 435, 2013. doi:10.1088/1742-6596/435/1/012041.

[39] J. Xia *et al.*, "Performance Analysis of Normality Test Loss for Intelligent RSCNN Denoiser Design With Application to Channel Decoding," in *2022 IEEE/CIC International Conference on Communications in China (ICCC)*, 2022, pp. 748–753. doi:10.1109/ICCC55456.2022.9880755.

[40] "Hypothesis testing for the inverse Gaussian distribution mean based on ranked set sampling," vol. 90, no. 13, pp. 2384–2394. doi:10.1080/00949655.2020.1777294.

[41] S. Bonovas and D. Piovani, "On p-Values and Statistical Significance," *J. Clin. Med.*, vol. 12, no. 3, p. 900, 2023. doi:10.3390/jcm12030900.

[42] M. Tsagris and N. Pandis, "Normality test: Is it necessary?," *Stat. Res. Des.*, vol. 159, no. 4, pp. 548–549, 2021. doi:10.1016/j.ajodo.2021.01.003.

[43] K. Ota, Q. Wu, P. Mamassian, and L. Maloney, "Visual cue estimation with non-gaussian distribution," *J. Vis.*, vol. 20, no. 11, p. 1436, 2020. doi:10.1167/jov.20.11.1436.

[44] J. Rodu and K. Kafadar, "The q–q Boxplot," *J. Comput. Graph. Stat.*, vol. 31, no. 1, pp. 26–39, 2022. doi:10.1080/10618600.2021.1938586.

[45] A. K. Yadav, K. Singh, and P. K. Srivastava, "Probabilistic Estimation of Comprehensive Utility Based on User Preference and Network Condition for Network Selection in Future in HetNet," *J. Supercomput.*, 2023. doi:10.1007/s11227-023-05595-4.

[46] E. Björnson; and L. Sanguinetti, "Rayleigh Fading Modeling and Channel Hardening for Reconfigurable Intelligent Surfaces," *IEEE Wirel. Commun. Lett.*, vol. 10, no. 4, pp. 830–834, 2020. doi:10.1109/LWC.2020.3046107.

[47] L. Klozar and J. Prokopec, "Propagation path loss models for mobile communication," *Proc. 21st Int. Conf. Radioelektronika 2011*, no. 2, pp. 1–4, Apr. 2011. doi:10.1109/RADIOELEK.2011.5936478.